Hindawi
Shock and Vibration
Volume 2023, Article ID 7731379, 11 pages
https://doi.org/10.1155/2023/7731379

Research Article

Sliding Mode Control of Ball Screw Meta-Action Unit Based on Disturbance Compensation and Inertia Identification

Hongyu Ge, Cangfu Wang, Chuanwei Zhang, and Manzhi Yang

School of Mechanical Engineering, Xi'an University of Science and Technology, Xi'an 710054, China

Correspondence should be addressed to Cangfu Wang; 21205224093@stu.xust.edu.cn

Received 8 May 2023; Revised 31 July 2023; Accepted 21 August 2023; Published 31 August 2023

Academic Editor: Francisco Beltran-Carbajal

To solve the problems of dynamic model parameter perturbation and external disturbances during the operation of the ball screw meta-action unit, an adaptive sliding mode control method based on disturbance compensation and inertia identification is proposed in this paper. First, a model of the ball screw meta-action unit is established and the dynamic equation is derived. Taking into account the uncertainty of the dynamic parameters, a least squares method with a forgetting factor is introduced to identify the moment of inertia in real time, and the identification results are utilized to adaptively adjust the sliding mode control law. Second, a nonlinear disturbance observer is designed to effectively observe the load disturbance, and the observed value is substituted into the sliding mode control as feedforward compensation to improve the anti-interference ability of the controller. Committed to the chattering of traditional sliding mode control, an improved adaptive exponential sliding mode reaching law is exploited to construct a novel sliding mode controller, thereby suppressing the slid mode chattering more thoroughly. Finally, the superiority of the proposed method is verified by MATLAB/Simulink simulation and compared with the other two control methods; the control method proposed in this paper can effectively improve the tracking performance of the system and has good robustness.

1. Introduction

Ball screw meta-action unit has been widely used in computer numerical control (CNC) machine tool, industrial robots, and other fields with the advantages of high precision, high efficiency, and high rigidity [1–3], and in particular, the transmission system of CNC machine tool with ball screw meta-action unit as the main driving unit is developing in the direction of high speed and high precision [4]. At the same time, with the development of the times, the accuracy of system control requirements is getting higher and higher. However, under actual operating conditions, due to the nonlinear characteristics of the system, the performance level of the ball screw meta-action unit control system is easily affected by parameter changes and external disturbances, and the traditional control algorithm has been difficult to achieve higher performance positioning and speed regulation [5–7].

To reduce the error generated in the feed movement and improve the reliability, various classic control methods have been used, e.g., gain scheduling (GS) control [8], adaptive control [9], active disturbance rejection control (ADRC) [10], and intelligence techniques, e.g., neural network control [11], H∞ control [12], and sliding mode control (SMC) [13]. Interestingly, SMC has the advantages of fast response to the system, less affected by internal and external interference and good robustness, which is widely used in the control system of mechanical units, but SMC often has chattering problem in practical applications [14–16]. Aiming at the problem of nonlinear speed regulation of permanent magnet synchronous motor control system, Wang et al. [17] designed an SMC method based on the new sliding mode reaching law to suppress chattering and improve the speed of reaching the sliding mode surface. Lu et al. [18] proposed a sinusoidal saturation function with variable boundary layer to suppress the chattering problem in the switching function. Huang et al. [19] proposed an adaptive SMC method based on the fuzzy exponential approach law to eliminate the unknown interference in the system and weaken the chattering of the system, but the setting of fuzzy rules requires a lot of experimental experience and is difficult to establish. In [20], an SMC method based on adaptive arrival law is proposed, the system state variables are combined with improved hyperbolic tangent function, to eliminate system chattering. However, when the perturbation of the system is large, the state variables of the system cannot guarantee a certain steady-state accuracy, and it is necessary to increase the gain of the switching function to reduce the impact of excessive disturbance on the steady-state accuracy of the system, but aggravate the chattering of the system, which limits the actual application of SMC. Therefore, how to improve the anti-interference ability of the system and the approach speed of the sliding mode surface as much as possible on the basis of weakening the chattering is a hot spot in current research.

In recent years, a series of advances have also been made in the study of using the idea of feed-forward compensation to solve system perturbations [21–23]. In [22], a new SMC method based on disturbance observer is proposed, the unknown disturbance is estimated by disturbance observer, and the nonlinear sliding mode surface is constructed from the estimated output value, which improves the robustness of the control system. Li proposed a composite control method based on extended state observer (ESO) and SMC and designed a third-order linear ESO to estimate the uncertain perturbation of the system, but in the design process of ESO, many parameters need to be selected, parameter setting is complicated, and the accuracy of interference estimation is limited [24]. Nonlinear disturbance observers (NDOs) have the advantages of a simple algorithm and easy engineering implementation and are widely used in disturbance compensation [25, 26]. Ding et al. [27] proposed an NDO-based terminal sliding mode control strategy, which used the observer to estimate the uncertainty perturbation in the system, thereby reducing the influence of perturbation on speed tracking. Nguyen et al. [28] designed a nonlinear perturbation observer that can self-adjust the gain of the observer and made effective estimates of the unmodeled parameters of the system and external perturbations, but the observed values fluctuated greatly. In the abovementioned methods, the motor parameters of the system are designed as observers with fixed values by default, and the real-time changes of the parameters are not considered. In [29], an identification method combined a Luenberger observer and the variable forgetting factor recursive least squares (FFRLS) method is proposed, but the results of parameter identification are not used in the design of the controller.

In summary, to improve the high-precision control of the ball screw meta-action unit control system, considering that the control system is susceptible to internal parameter changes and external interference, an adaptive SMC method based on disturbance compensation and inertia identification is proposed. First, this paper designs an adaptive sliding mode reaching law based on system state variables and tracking error and its reaching law gain term will change with the change of system state variables, which can not only self-adjust the approach speed but also reduce the sliding mode chattering. Second, the NDO is designed to estimate the external disturbance and parameter uncertainty in real time, and the observed value is introduced into the design of the controller as compensation, and considering the real-time change of the motor moment of inertia, the moment of inertia is identified by FFRLS method, so as to improve the estimation accuracy of the observer and the anti-interference performance of the controller.

2. Building of Ball Screw Meta-Action Unit Model

2.1. Physical Model of Ball Screw Meta-Action Unit. To fully reflect the characteristics of "motion" and motion-related characteristics of the system in the drive system of CNC machine tool, this paper uses meta-motion theory to build the frame of CNC machine tool feed system, chooses the most common ball screw meta-action unit system as the research object, and studies the control performance of ball screw meta-action unit from the angle of force and torque transmission. As shown in Figure 1, the entire consisting of all components (inputs, execution piece, middleware, supports, and fasteners) according to the assembly relationship is called the meta-action unit [30].

The meta-action unit of the ball screw is composed of an input part (motor), a middle part (coupling and ball screw), a fastener (left bearing and right bearing and nut), an output part (worktable), and a support part (guide rail and base), as shown in Figure 2.

The motion form of the action unit platform of the ball screw is mainly through the rolling body circulating back and forth between the lead screw raceway and the nut raceway to carry out the spiral motion, thus realizing the transformation of the rotary motion of the lead screw into the linear motion of the nut, the nut drives the worktable to realize the linear feed movement and, finally, realizes the feed movement of the actuator through the transmission of force or torque.

2.2. Dynamic Modeling of Ball Screw Meta-Action Unit. The transmission parts of the ball screw meta-action unit are not ideal rigid body, and the input and the actuator are often connected by elastic elements or flexible parts, so in this paper, the transmission ball screw is regarded as a flexible body because the transmission itself has a small moment of inertia, can be ignored, with transmission stiffness and damping coefficient to describe, after simplification, the entire drive system of the ball screw meta-action unit which can be regarded as a motor-load composed of the dual-mass system model, as shown in Figure 3. According to the model of the system, the dynamic equation is [31]

$$\begin{aligned} T_m &= J_m \ddot{\theta}_m + b_m \dot{\theta}_m + T_s, \\ T_s &= k_s (\theta_m - \theta_l) + b_s (\dot{\theta}_m - \dot{\theta}_l), \\ T_l &= T_s - J_l \ddot{\theta}_l - b_l \dot{\theta}_l, \end{aligned} \tag{1}$$

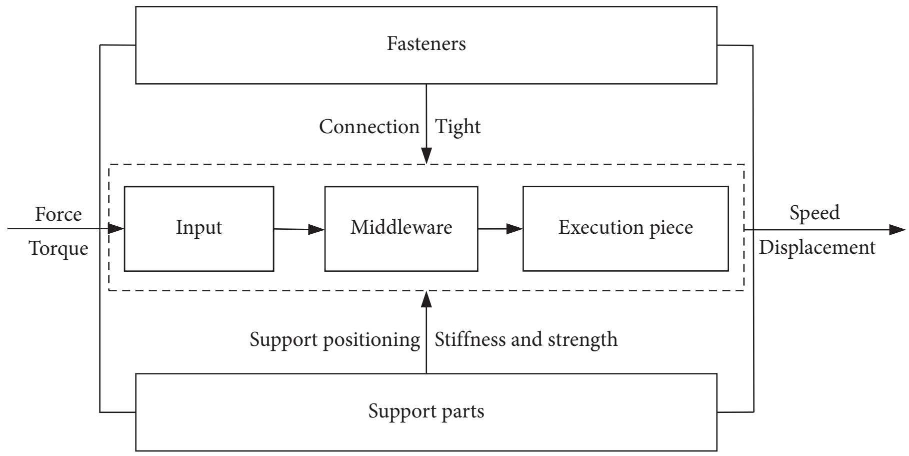

FIGURE 1: Schematic diagram of meta-action unit structure.

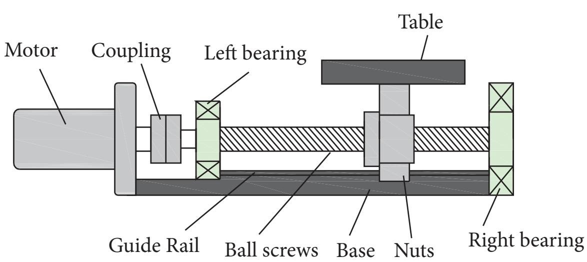

FIGURE 2: Ball screw meta-action unit platform.

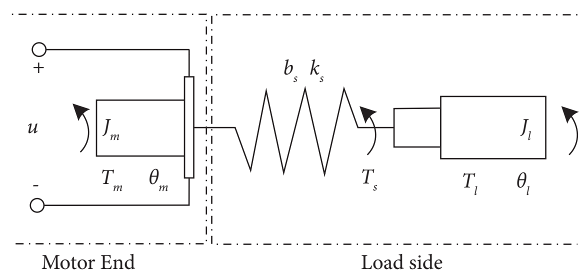

FIGURE 3: The dual-mass system.

where T_m is the control torque of the servo motor, J_m is the motor moment of inertia, b_m is the motor damping coefficient, b_l is the damping constants of the load, T_s is the transmission torque of the propeller shaft, T_l is the load torque, J_l is the equivalent moment of inertia of the load, k_s is the equivalent stiffness of the flexible element, b_s is the damping coefficient of the flexible element, and θ_m and θ_l are the equivalent output angles of the motor shaft and the table.

To make the ball screw meta-action unit have good tracking accuracy and improve the tracking performance of the system, it is necessary to design the control strategy according to the established dynamic model. The control goal of this paper is to design an adaptive sliding mode controller to ensure that the system position output can quickly and stably track the desired trajectory.

3. Sliding Mode Control Design Based on Nonlinear Disturbance Observer

3.1. Design of Control Laws. SMC is essentially a nonlinear control, that is, the control structure changes with time [32] because SMC is not sensitive to parameter disturbance and is often used for the control of nonlinear systems, so this paper adopts the SMC strategy to achieve system tracking control.

According to equation (1), defining $x = (x_1, x_2, x_3, x_4)^T = (\theta_m, \dot{\theta}_m, \theta_l, \dot{\theta}_l)^T$, we can obtain the equation of motion of the state of the ball screw meta-action unit:

$$\begin{cases} \dot{x} = f(x) + \mathrm{gu} + d, \\ y = h(x). \end{cases} \tag{2}$$

$$f(x) = \begin{bmatrix} x_2 \\ -\dfrac{1}{J_m}\left(b_m x_2 + J_l \dot{x}_4 + b_l x_4\right) \\ x_4 \\ \dfrac{1}{J_l}\left(T_s - b_l x_4\right) \end{bmatrix},$$

$$g = \begin{bmatrix} 0 \\ \dfrac{1}{J_m} \\ 0 \\ 0 \end{bmatrix}, \tag{3}$$

$$d = \begin{bmatrix} 0 \\ -\dfrac{T_l}{J_m} \\ 0 \\ -\dfrac{T_l}{J_l} \end{bmatrix},$$

$$h(x) = x_2,$$

where $u = T_m$ is the control input of the system, expressed as electromagnetic torque in the physical sense, and x_2 is the output variable of the system.

We also define the sliding mode function as

$$s = ce + \dot{e}, \tag{4}$$

where $e = x_1 - x_d$ (x_d is the reference signal) is the tracking error, $c > 0$, and satisfies the Hurwitz polynomial condition.

Finding the first derivative of s and combining equation (2) yields

$$\dot{s} = c\dot{e} + e = c(x_2 - \dot{x}_d) + \dot{x}_2 - \ddot{x}_d = cx_2 - c\dot{x}_d - x_d + f_2(x) + gu + d_2, \tag{5}$$

where $f_2(x) = -1/J_m(b_m x_2 + J_l \dot{x}_4 + b_l x_4), d_2 = -T_l/J_m$.

For SMC, to improve the convergence speed of the system and weaken the chattering, the exponential reaching law is selected:

$$\dot{s} = -ks - \varepsilon sgn(s), \tag{6}$$

where $k > 0, \varepsilon > 0$, where k and ε are positively correlated with the sliding mode approach velocity and the sliding mode chattering, respectively. Generally speaking, in the process of selecting SMC parameters, the k value should be made as large as possible to speed up the reaching speed, and the ε value should be selected as small as possible to reduce sliding mode chattering.

In fact, the values of k and ε are difficult to select or include in the uncertain parameter boundary, so in order to solve this problem, this paper adopts the improved adaptive exponential sliding mode approximation law, so that the systematic tracking error variable is associated with the sliding mode reaching law, so as to improve the adaptive ability of SMC, and the improved adaptive exponential sliding mode reaching law is as follows:

$$\begin{cases} \dot{s} = -ks - \dfrac{\varepsilon}{N}|e|\text{sgn}(s), \\ \lim\limits_{n\longrightarrow\infty} |e| = 0, \\ N = \rho + (1-\rho)e^{-\beta_0 |s|\gamma_0}, \end{cases} \tag{7}$$

where $0 < \rho < 1, \beta_0 > 0, \gamma_0 > 0$ and e is the tracking error.

From equation (7), when $|s|$ tends to ∞, $N = \rho$, and $\dot{s} = -ks - \varepsilon/\rho|e|\text{sgn}(s), \varepsilon/\rho > \varepsilon$, at this time, the reaching law has a faster reaching speed and when $|s|$ tends to 0 and $N = 1$, the reaching law is close to the conventional exponential reaching law. The gain term of the reaching law can be dynamically adjusted with the changes of the sliding surface and system state. When the state error is large, the reaching speed is increased, and when the state error is small and close to the sliding mode surface, the chattering level of the system is reduced by reducing the approach speed.

Combining equations (3), (5), and (7) yields the following adaptive control law:

$$u = \frac{(c(\dot{x}_d - x_2) + \ddot{x}_d - ks - (\varepsilon/N)|e|\text{sgn}(s) - f_2(x) - d_2)}{g}. \tag{8}$$

3.2. Design of Nonlinear Disturbance Observers. To improve the anti-interference ability and control accuracy of the system, NDO is used to estimate interference and compensate it into the control law as a feed-forward term to improve the robustness of SMC [33]. Here, we mainly consider the system load transmission torque T_l as an external disturbance and then consider using an observer to estimate and compensate for this.

From equation (3), the equation of motion of the system can be expressed as

$$d_2 = \ddot{x}_1 - \text{gu} - f_2(x). \tag{9}$$

Then, the design observer is

$$\dot{\hat{d}}_2 = l(d_2 - \hat{d}_2) = l(\ddot{x}_1 - \text{gu} - f_2(x)) - l\hat{d}_2, \tag{10}$$

where l is the observer gain and $\hat{d}_2$ is the observed value of interference.

We define the observation error as

$$\tilde{d}_2 = d_2 - \hat{d}_2. \tag{11}$$

Since the frequency of d_2 change is low relative to the dynamic characteristics of the observer and the sampling frequency of the system, it can be assumed that $\dot{d}_2 = 0$. We derive equation (11) and substitute it into equation (10), and the dynamics of the observation error can be described in the following equation:

$$\dot{\tilde{d}}_2 + l\tilde{d}_2 = 0. \tag{12}$$

As can be seen from equation (12), when l is positive, the observer gain l can be designed so that the observation error $\tilde{d}_2$ converges exponentially to 0, the convergence speed is positively correlated with l, and when l is large, it will cause fluctuations in the system, and the convergence speed will slow down when l is running at a low speed, so when the system is running at a low speed, a larger l should be selected, and when the system is running at a high speed, a smaller l should be selected to reduce the oscillation of the system.

However, due to the influence of noise signals during measurement, the acceleration signal $\ddot{x}_1$ is difficult to obtain, so the designed observer needs to be reconstructed to define an intermediate variable as

$$z = \hat{d}_2 - p(\dot{x}_1). \tag{13}$$

Let $p(\dot{x}_1) = l\dot{x}_1$, the derivation of equation (13) and substitution into equation (10), be obtained

$$\begin{aligned}\dot{z} &= \dot{\widehat{d}}_2 - \dot{p}(\dot{x}_1) = l(\ddot{x}_1 - gu - f_2(x)) - l\widehat{d}_2 - l\ddot{x}_1 \\ &= -l\widehat{d}_2 - l(gu + f_2(x)).\end{aligned} \tag{14}$$

The NDO constructed by equations (13) and (14) is

$$\begin{cases}\dot{z} = -lz - l[p(\dot{x}_1) + \mathrm{gu} + f_2(x)], \\ \widehat{d}_2 = z + p(\dot{x}_1).\end{cases} \tag{15}$$

If the perturbation observation $\widehat{d}_2$ is introduced into the designed SMC, the new control law is

$$u = \frac{\left(c(\dot{x}_d - x_2) + \ddot{x}_d - ks - (\varepsilon/N)|e|\mathrm{sgn}(s) - f_2(x) - \widehat{d}_2\right)}{g}. \tag{16}$$

To verify the stability of the designed controller, the Lyapunov function is selected as

$$V = \frac{1}{2}s^2 + \frac{1}{2}\widetilde{d}_2^{\,T}\widetilde{d}_2. \tag{17}$$

The first derivative of equation (17) is obtained and brought into equations (7) and (12).

$$\dot{V} = s\dot{s} + \widetilde{d}_2^{\,T}\dot{\widetilde{d}}_2 = s(cx_2 - c\dot{x}_d - \ddot{x}_d + f_2(x) + \mathrm{gu} + d_2) - l\widetilde{d}_2^{\,T}\widetilde{d}_2. \tag{18}$$

Substituting the control law (16) into equation (18), we can obtain the following equation:

$$\begin{aligned}\dot{V} &= s\left(-ks - \frac{\varepsilon}{N}|e|sgn(s) - \widetilde{d}_2\right) - l\widetilde{d}_2^{\,2} \\ &= -ks^2 - \frac{\varepsilon}{N}|e||s| - s\widetilde{d}_2 - l\widetilde{d}_2^{\,2} \\ &\leq -ks^2 - \left(\frac{\varepsilon}{N}|e| + |\widetilde{d}_2|\right)|s| - l\widetilde{d}_2^{\,2}.\end{aligned} \tag{19}$$

According to equation (7), $k > 0, \varepsilon > 0, \rho \leq N \leq 1$, and $\varepsilon/\rho < \varepsilon/N < \varepsilon$. It is proved by stability that when l is positive, finally $\dot{V} \leq 0, V \geq 0$.

It can be seen that both the sliding surface s and the observation error $\widetilde{d}_2$ will converge in a limited time, that is, the designed system is progressively stable.

3.3. Identification of Rotational Inertia. In the design of the abovementioned controller, the rotational inertia J_m is regarded as a fixed value, but because the ball screw meta-action unit is a complex system with time-varying characteristics, the moment of inertia will change with running time, seriously affecting the robustness of the controller, so this paper mainly uses the FFRLS method to identify the system uncertainty parameter J_m and real-time feedback to the SMC law to improve the anti-interference ability of the system.

From equations (1)–(3), it can be deduced that the transfer function from the control input u to the motor output variable y is

$$G(s) = \frac{y}{u} = \frac{\left(J_l s^2 + b_s s + k_s\right)}{\left(J_m J_l s^3 + (J_m + J_l)b_s s^2 + (J_m + J_l)k_s s\right)}. \tag{20}$$

In this paper, bilinear transformation is used to discretize the transfer function, and finally, a recursive expression based on least square form is established.

Here, $s = 2/T \bullet (1 - z^{-1})/(1 + z^{-1})$, let T be the sampling period, and we process equation (20) to obtain

$$\begin{aligned}\frac{y}{u} &= \frac{J_l\left(2/T \bullet 1 - z^{-1}/1 + z^{-1}\right)^2 + b_s\left(2/T \bullet 1 - z^{-1}/1 + z^{-1}\right) + k_s}{J_m J_l\left(2/T \bullet 1 - z^{-1}/1 + z^{-1}\right)^3 + b_s(J_m + J_l)\left(2/T \bullet 1 - z^{-1}/1 + z^{-1}\right)^2 + k_s(J_m + J_l)\left(2/T \bullet 1 - z^{-1}/1 + z^{-1}\right)} \\ &= \frac{2}{T} \bullet \frac{\left(A_0 + A_1 z^{-1} + A_2 z^{-2} + A_3 z^{-3}\right)}{\left(B_0 + B_1 z^{-1} + B_2 z^{-2} + B_3 z^{-3}\right)}.\end{aligned} \tag{21}$$

In equation (21),

$$\begin{cases} A_0 = 4J_l + 2b_sT + k_sT^2, \\ A_1 = -4J_l + 2b_sT + 3k_sT^2, \\ A_2 = -4J_l - 2b_sT + 3k_sT^2, \\ A_3 = 4J_l - 2b_sT + k_sT^2, \\ B_0 = 4J_lJ_m + 2b_s(J_m + J_l)T + k_s(J_m + J_l)T^2, \\ B_1 = -12J_lJ_m - 2b_s(J_m + J_l)T + k_s(J_m + J_l)T^2, \\ B_2 = 12J_lJ_m - 2b_s(J_m + J_l)T - k_s(J_m + J_l)T^2, \\ B_3 = -\left[4J_lJ_m - 2b_s(J_m + J_l)T + k_s(J_m + J_l)T^2\right]. \end{cases} \tag{22}$$

From equation (22), the recurrence formula is obtained:

$$y(k) = \frac{T}{2}\left[\frac{A_0}{B_0}\bullet u(k) + \frac{A_1}{B_0}\bullet u(k-1) + \frac{A_2}{B_0}\bullet u(k-2) + \frac{A_3}{B_0}\bullet u(k-3)\right] - \left[\frac{B_1}{B_0}\bullet y(k-1) + \frac{B_2}{B_0}\bullet y(k-2) + \frac{B_3}{B_0}\bullet y(k-3)\right], \tag{23}$$

where $u(k)$ and $y(k)$ are the measured data of the input and output at time k, respectively.

By performing a Z-inverse transformation of the discrete transfer function, the autoregressive moving average model in the time domain can be obtained as follows:

$$y(k) = \varphi(k)^T\theta. \tag{24}$$

Equation (24) is the least square form of the discretized difference equation. Combining equations (23) and (24), it can be obtained that the parameter vector and the vector to be estimated are

$$\varphi(k) = \begin{bmatrix} u(k), u(k-1), u(k-2), u(k-3) \\ -y(k-1), -y(k-2), -y(k-3) \end{bmatrix}^T,$$
$$\theta = \left[\frac{T}{2}\bullet\frac{A_0}{B_0}, \frac{T}{2}\bullet\frac{A_1}{B_0}, \frac{T}{2}\bullet\frac{A_2}{B_0}, \frac{T}{2}\bullet\frac{A_3}{B_0}, \frac{B_1}{B_0}, \frac{B_2}{B_0}, \frac{B_3}{B_0}\right]. \tag{25}$$

As can be seen from equation (25), the parameter vector contains seven parameters that need to be fitted, and the relationship between them is as follows:

$$\begin{aligned} \theta_1 + \theta_2 &= \frac{T}{2}\bullet\frac{4\left(b_sT + k_sT^2\right)}{4J_lJ_m + 2(J_m + J_l)T + k_s(J_m + J_l)T^2}, \\ \theta_2 - \theta_3 &= \frac{T}{2}\bullet\frac{4b_sT}{4J_lJ_m + 2(J_m + J_l)T + k_s(J_m + J_l)T^2}, \\ \theta_2 + \theta_4 &= \frac{T}{2}\bullet\frac{4k_sT^2}{4J_lJ_m + 2(J_m + J_l)T + k_s(J_m + J_l)T^2}, \\ \theta_5 + \theta_7 &= \frac{T}{2}\bullet\frac{16J_lJ_m}{4J_lJ_m + 2(J_m + J_l)T + k_s(J_m + J_l)T^2}. \end{aligned} \tag{26}$$

Combined with the N discrete instantaneous sampling values of the input quantity $u(k)$ and the output $y(k)$ in the estimation vector $\varphi(k)$, the input and output values are fitted to the form of (23) to find the parameter vector θ, and then the equivalent relationship between the parameters of equation (26) is used as the solution set, and finally, the fsolve toolbox of MATLAB can be used to find four unknowns with unique solutions $\hat{J}_m, \hat{J}_l, \hat{b}_s, \hat{k}_s$. In order to realize the real-time update of J_m, this paper only identifies the parameter of the motor moment of inertia $\hat{J}_m$.

Furthermore, FFRLS is used to identify the estimated parameters. The FFRLS formula is as follows:

$$\begin{aligned} \hat{\theta}(k) &= \hat{\theta}(k-1) + K(k)\left[y(k) - \varphi^T(k)\hat{\theta}(k-1)\right], \\ K(k) &= \frac{P(k-1)\varphi(k)}{\lambda + \varphi^T(k)P(k-1)\varphi(k)}, \\ P(k) &= \frac{1}{\lambda(k)}\left[I - K(k)\varphi^T(k)\right]P(k-1), \end{aligned} \tag{27}$$

where $\hat{\theta}(k)$ expressed as an estimation vector of the identification parameter at k-time, $\hat{\theta}(k-1)$ represents the observed value of the system output at the $k-1$ th moment, $y(k)$ represents the actual output of the system, $\varphi(k)$ represents the observation matrix of the system at the k th moment, $K(k)$ represents the estimated gain matrix of the system, $P(k-1)$ represents the error covariance matrix of the system, and λ is the forgetting factor.

At this point, the identified $\hat{J}_m$ is updated to the SMC designed in this paper, and the new control law is

$$u = \frac{1}{\hat{g}}\left(c(\dot{x}_d - x_2) + \ddot{x}_d - ks - \frac{\varepsilon}{N}|e|\text{sgn}(s) - f_2(x) - \hat{d}_2\right). \tag{28}$$

4. Simulation Results and Discussion

For the purpose of verifying the proposed algorithms, this section conducts simulation verification using MATLAB/ Simulink. Table 1 shows the mechanical structure parameters of the ball screw meta-action unit.

Table 1: Mechanical structural parameters of the ball screw meta-action unit.

Parameters	Values
J_m	$0.0017\,\mathrm{kg\cdot m^2}$
J_l	$0.0014\,\mathrm{kg\cdot m^2}$
b_m	$0.042\,\mathrm{N\cdot m\cdot s}$
b_l	$0.05\,\mathrm{N\cdot m\cdot s}$
k_s	$630\,\mathrm{N\cdot m/rad}$
b_s	$0.005\,\mathrm{N\cdot m\cdot s}$

4.1. Parameter Identification Simulation Analysis. The specific simulation parameters of the system are shown in Table 1. The sampling period T is 0.0001 s, and the input signal uses white noise. With the increase of the data amount during the system operation, the value of $K(k)$ and $P(k)$ in equation (27) will decrease with the increase of the data, and the correction ability of the observed value $\widehat{\theta}(k)$ output by the system will become smaller and smaller, leading to the phenomenon of "data saturation" of the system.

The least square method with forgetting factor avoids the rapid decline of adaptive gain and overcomes this phenomenon by introducing a forgetting factor in parameter identification. In the simulation, the forgetting factor λ is selected as 0.95, and the simulation time is selected as 1 s. The identification results are shown in Figure 4.

In Figure 4, the red dashed line represents the true value of the system parameters, and the blue solid line represents the estimated value obtained from identification. The results in the figure indicate that when the forgetting factor λ is selected as 0.95, the motor's moment of inertia can converge to the true value at 0.063 seconds and is basically stable around $0.0017\,\mathrm{kg\bullet m^2}$.This indicates that the least squares method with forgetting factors can effectively identify the required parameters.

4.2. Simulation Analysis of Control Effect. In this section, the following three SMC methods will be selected to verify the effectiveness of the proposed adaptive SMC algorithm based on disturbance compensation and inertia recognition, and the simulation and comparison results are shown in Figures 5–8.

(1) In the control method based on the traditional sliding mode reaching law (SMC), the reaching law is $\dot{s} = -ks - \varepsilon|s|^{\sigma}\mathrm{sgn}(s)$, where the controller parameters are set to $\varepsilon = 0.005, k = 30, \sigma = 0.1$

(2) Parameters of traditional sliding mode controllers based on nonlinear disturbance observers (NDO + SMC) are $\varepsilon = 0.005, k = 30, c = 20$

(3) This paper designs the parameters required for an adaptive SMC algorithm based on disturbance compensation and inertia identification: $\varepsilon = 0.005$, $k = 30, c = 20, \rho = 0.65, \beta_0 = 15, \gamma_0 = 10$

First, the estimation capability of NDO is verified by simulation, and its curve is shown in Figure 5, from which it can be seen that under the condition of $T_l = 10\mathrm{N\bullet m}$ for a given load torque, the observer can stably estimate the actual external disturbance, which effectively improves the anti-interference ability of the system.

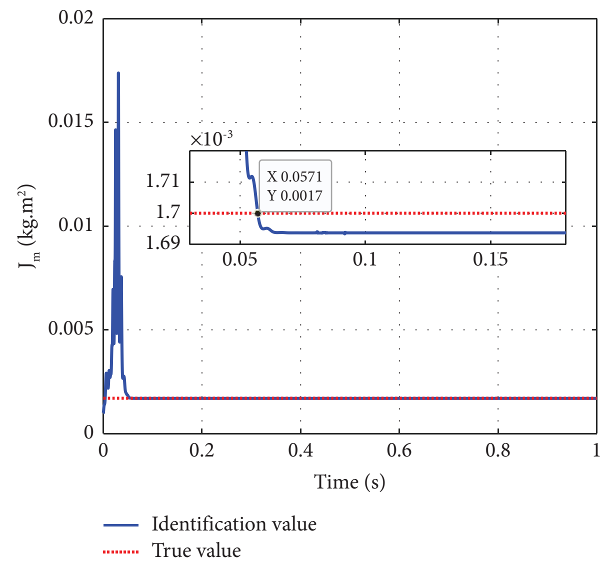

Figure 4: Identification results of motor rotational inertia.

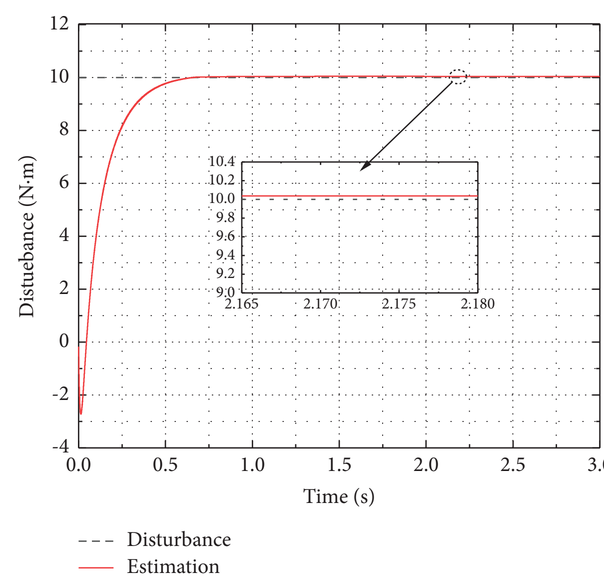

Figure 5: Simulation results of load disturbance observer.

Second, two different signals are set as reference instructions and the control strategy is simulated and verified.

The first case is that the simulation time is set to 3 s, and the results are shown in Figure 6. From Figure 6(a), it can be seen that the method proposed in this paper has good convergence speed and tracking performance. Figure 6(b) is a comparison diagram of the tracking error change rate of the three controllers, which shows that the method proposed in this paper has a faster error convergence rate than the other two controllers. When the system reaches a steady state, the steady-state error rate of the method proposed in this paper is small, and the other two methods have a large change rate. Figure 6(c) is a comparative diagram of the

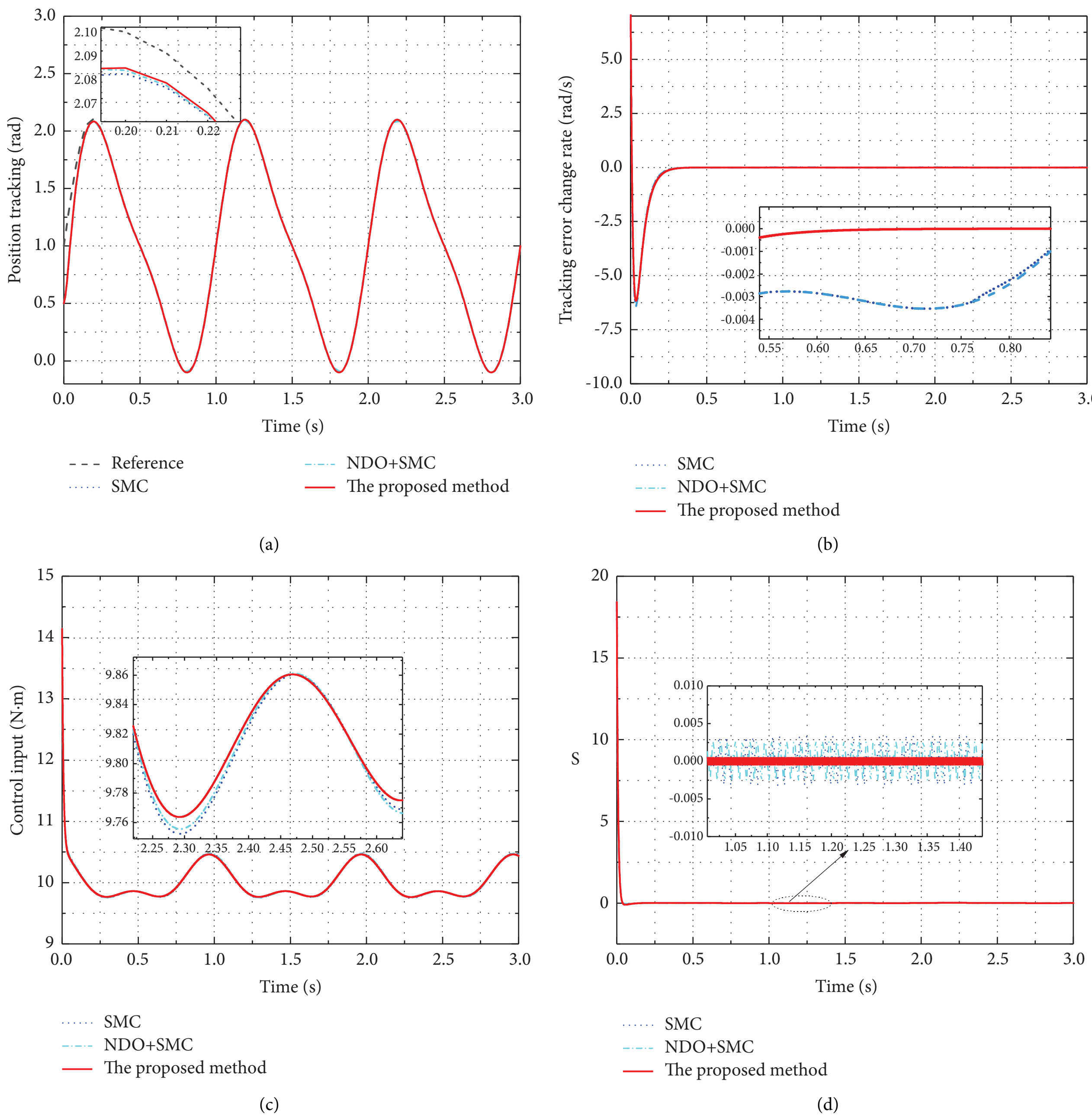

FIGURE 6: Simulation results of trajectory at $x_d = 1 + \sin(2\pi t) + 0.25\sin(4\pi t)$. (a) Position tracking. (b) Tracking error change rate. (c) Control input. (d) Comparison of the sliding mode function curves.

control input curve, from which it can be seen that the control method designed herein requires less control than the other two methods. Figure 6(d) is a sliding mode curve comparison chart of the three methods; compared with the other two methods, the control method in this paper can realize the adaptive ability of the sliding mode reaching law and adaptively adjust the switching gain, and at the same time, the disturbance observer compensates for the influence of partial disturbance on the system, thereby reducing the sliding mode chattering.

In the second case, to further verify the superior performance of the proposed algorithm and to consider the impact of system disturbances, the reference signal is set to $x_d = 1$, and the simulation time is also set to 3 s. When running for 2 s, we add controller interference $n = 0.8\sin(\pi t)$, at which point the system can be represented as

$$\begin{cases} \dot{x} = f(x) + g(u + n) + d, \\ h = h(x). \end{cases} \quad (29)$$

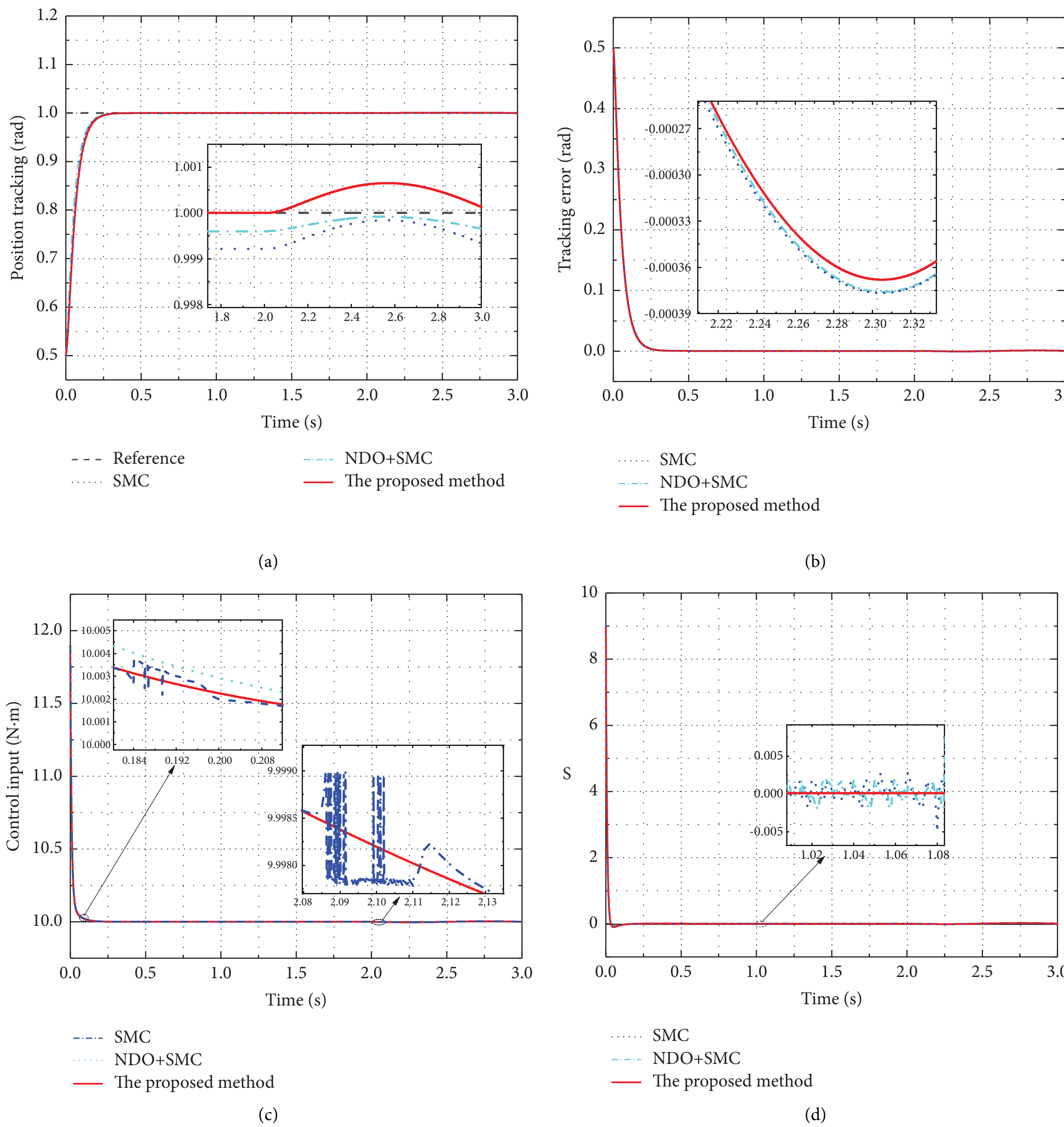

Figure 7: Simulation results of trajectory at $x_d = 1$. (a) Position tracking. (b) Tracking error. (c) Control input. (d) Comparison of the sliding mode function curves.

The simulation signal results are shown in Figure 7. It can be seen from the figure that the control method in this paper still has a good tracking effect after suddenly adding a disturbance signal. Figure 7(b) is a comparison of the tracking error of the three controllers after a burst perturbation. It can be seen that the maximum error of the proposed method is smaller than the maximum error of the other two control methods, and the error under the proposed method can be restored to a stable state in a relatively short time. It can be seen that the method in this paper has better and superior performance. It can be seen in Figure 7(c) that the input signal of the control method proposed in this paper is relatively smooth and there is no high-frequency chattering phenomenon, which indicates that the designed method can effectively avoid the chattering problem of traditional SMC. Figure 7(d) shows the sliding mode curve comparison chart of different algorithms, and it can be further seen that the proposed method has a good effect on weakening chattering.

In addition, in the third case, the system response when the load inertia J_l changes is studied. Given the required input instruction $x_d = 1$, starting load inertia $J_l = 0.0014\,\mathrm{kg{\cdot}}m^2$; when the system runs for 1 s, J_l increased to $J_l = 0.0028\,\mathrm{kg} \bullet m^2$; the simulation comparison diagram is

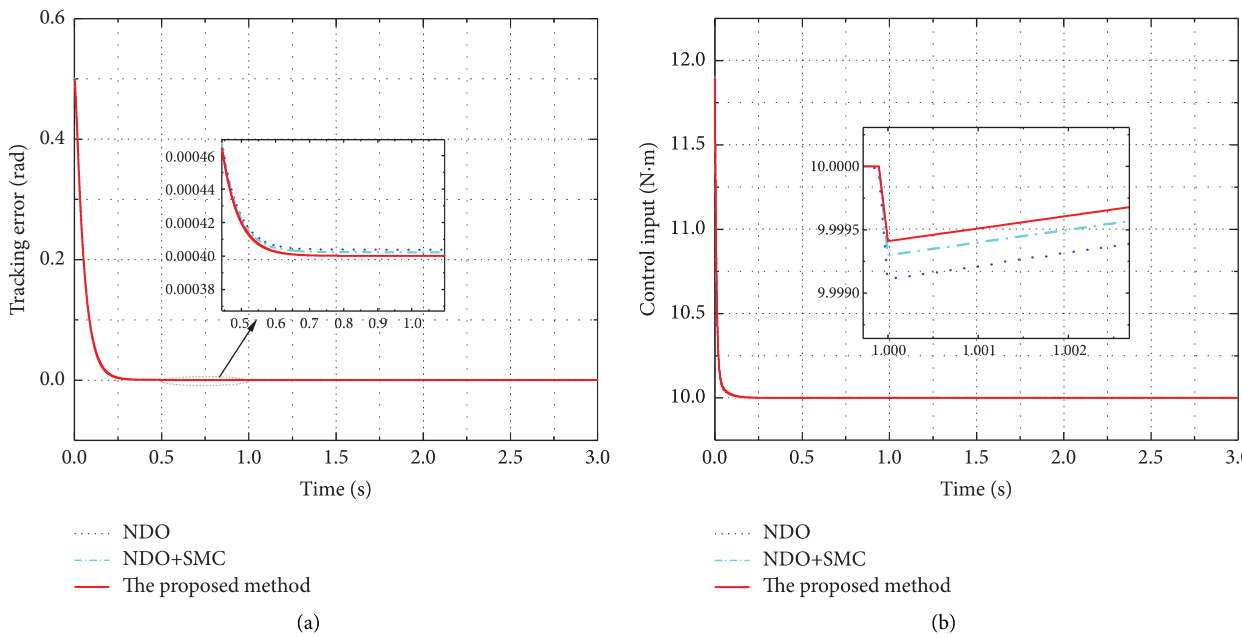

FIGURE 8: Trajectory simulation results at $x_d = 1$ under J_l mutation. (a) Tracking error. (b) Control input.

shown in Figure 8; from Figure 8(a), it can be seen that, in the case of sudden J_l, the tracking error of the algorithm designed in this paper is still small compared to the other two control methods, effectively improving the tracking performance of the system; Figure 8(b) is the control input diagram of J_l before and after the mutation; it can be seen that when J_l is mutated in 1 s, the control algorithm required in this paper requires a smaller amount of control. The influence of chattering is reduced, indicating that the method designed in this paper can effectively cope with parameter change.

5. Conclusions

In this paper, an adaptive SMC method based on disturbance compensation and inertia identification is proposed, and an adaptive sliding mode approximation law based on system variables is designed, and the gain term of the reaching law is adjusted online through adaptive adjustment technology, which weakens the sliding mode chattering and improves the adaptive ability of reaching speed. To further improve the anti-interference ability and steady-state performance of the system, an NDO is designed to estimate the load disturbance of the system. Considering that the moment of inertia will change with time, FFRLS is used to identify the moment of inertia online, so that the moment of inertia is more flexible. Finally, the effectiveness of the proposed method is verified by simulation, and the control method can better improve the steady-state performance and the ability to suppress disturbances by comparing with other control methods.

Data Availability

The data used in this study are mathematical-based simulations and are available from the corresponding author upon reasonable request.

Conflicts of Interest

The authors declare that they have no conflicts of interest.

Acknowledgments

This work was funded by the National Natural Science Foundation of China, No. 51705417.

References

[1] S. Wang, J. Na, and Y. Xing, "Adaptive optimal parameter estimation and control of servo mechanisms: theory and experiments," *IEEE Transactions on Industrial Electronics*, vol. 68, no. 1, pp. 598–608, 2021.

[2] J. Yao and W. Deng, "Active disturbance rejection adaptive control of hydraulic servo systems," *IEEE Transactions on Industrial Electronics*, vol. 64, no. 10, pp. 8023–8032, 2017.

[3] X. Gao, X. Zhang, J. Yang, Z. Fu, M. Wang, and T. Zan, "Dynamic modeling and analysis on lateral vibration of ball screw feed system," *The International Journal of Advanced Manufacturing Technology*, vol. 124, no. 11-12, pp. 4211–4229, 2023.

[4] T. Huang, Y. T. Kang, S. J. Du et al., "A survey of modeling and control in ball screw feed-drive system," *The International Journal of Advanced Manufacturing Technology*, vol. 121, no. 5-6, pp. 2923–2946, 2022.

[5] C. N. Cho, C. H. Lee, and H. J. Kim, "Disturbance observer and error model-based control of ball screw drives," *Journal of The Korean Society of Industry Convergence*, vol. 22, no. 4, pp. 435–445, 2019.

[6] D. F. Bao, W. C. Tang, and L. Dong, "Integral sliding mode control for flexible ball screw drives with matched and mismatched uncertainties and disturbances," *Journal of Central South University*, vol. 24, no. 9, pp. 1992–2000, 2017.

[7] M. Hanifzadegan and R. Nagamune, "Tracking and structural vibration control of flexible ball-screw drives with dynamic

variations," *Ieee-Asme Transactions on Mechatronics*, vol. 20, no. 1, pp. 133–142, 2015.

[8] L. Zhang, J. H. Liu, C. B. Zhuang, M. Q. Yao, F. H. Chen, and C. Y. Zhang, "Gain scheduling control of ball screw feed drives based on linear parameter varying model," *The International Journal of Advanced Manufacturing Technology*, vol. 124, no. 11-12, pp. 4493–4510, 2023.

[9] N. Wang and M. J. Er, "Direct adaptive fuzzy tracking control of marine vehicles with fully unknown parametric dynamics and uncertainties," *IEEE Transactions on Control Systems Technology*, vol. 24, no. 5, pp. 1845–1852, 2016.

[10] C. Zhang and Y. Chen, "Tracking control of ball screw drives using ADRC and equivalent-error-model-based feedforward control," *IEEE Transactions on Industrial Electronics*, vol. 63, no. 12, pp. 7682–7692, 2016.

[11] R. K. Vashisht and Q. Peng, "Online chatter detection for milling operations using LSTM neural networks assisted by motor current signals of ball screw drives," *Journal of Manufacturing Science and Engineering*, vol. 143, no. 1, 2020.

[12] H. Dong, Z. Wang, S. X. Ding, and H. Gao, "On H-infinity estimation of randomly occurring faults for A class of nonlinear time-varying systems with fading channels," *IEEE Transactions on Automatic Control*, vol. 61, no. 2, pp. 479–484, 2016.

[13] L. Dong and W. C. Tang, "Adaptive backstepping sliding mode control of flexible ball screw drives with time-varying parametric uncertainties and disturbances," *ISA Transactions*, vol. 53, no. 1, pp. 110–116, 2014.

[14] M. Neubauer, F. Brenner, C. Hinze, and A. Verl, "Cascaded sliding mode position control (SMC-PI) for an improved dynamic behavior of elastic feed drives," *International Journal of Machine Tools and Manufacture*, vol. 169, Article ID 103796, 2021.

[15] H. H. Lin, M. Y. Cheng, Y. T. Chen, and C. Y. Huang, "Contour following accuracy improvement-A dynamic fast nonsingular terminal sliding mode control approach," *IEEE Access*, vol. 10, pp. 34185–34195, 2022.

[16] L. Zhao, X. Y. Cao, and X. F. Li, "Adaptive sliding-mode control for inertial reference units via adaptive tracking differentiators," *IEEE Transactions on Systems, Man, and Cybernetics: Systems*, vol. 53, no. 5, pp. 3208–3218, 2023.

[17] Y. Q. Wang, Y. T. Feng, X. G. Zhang, and J. Liang, "A new reaching law for antidisturbance sliding-mode control of PMSM speed regulation system," *IEEE Transactions on Power Electronics*, vol. 35, no. 4, pp. 4117–4126, 2020.

[18] X. Lu, H. Lin, Y. Feng, and J. Han, "Soft switching sliding mode observer for PMSM sensorless control," *Diangong Jishu Xuebao/Transactions of China Electrotechnical Society*, vol. 30, no. 2, pp. 106–113, 2015.

[19] C. L. Huang, T. Wang, M. Li, and Y. Yu, "Sliding mode control of servo feed system based on fuzzy reaching law," *Applied Sciences*, vol. 13, no. 10, p. 6086, 2023.

[20] X. Zhang and Y. Quan, "Adaptive fractional-order nonsingular fast terminal sliding mode control based on fixed time disturbance observer for manipulators," *IEEE Access*, vol. 10, pp. 76504–76511, 2022.

[21] K. Cho, J. Kim, S. B. Choi, and S. Oh, "A high-precision motion control based on a periodic adaptive disturbance observer in a PMLSM," *IEEE*, vol. 20, pp. 2158–2171, 2015.

[22] N. Ahmed and M. Chen, "Sliding mode control for quadrotor with disturbance observer," *Advances in Mechanical Engineering*, vol. 10, no. 7, Article ID 168781401878233, 2018.

[23] J. Gil, S. You, Y. Lee, and W. Kim, "Nonlinear sliding mode controller using disturbance observer for permanent magnet synchronous motors under disturbance," *Expert Systems with Applications*, vol. 214, Article ID 119085, 2023.

[24] L. Cui, N. Jin, S. Chang, Z. Zuo, and Z. Zhao, "Fixed-time ESO based fixed-time integral terminal sliding mode controller design for a missile," *ISA Transactions*, vol. 125, pp. 237–251, 2022.

[25] M. Alipour, J. Zarei, R. Razavi-Far, M. Saif, N. Mijatovic, and T. Dragicevic, "Observer-based backstepping sliding mode control design for microgrids feeding a constant power load," *IEEE Transactions on Industrial Electronics*, vol. 70, no. 1, pp. 465–473, 2023.

[26] R. Ma, H. Zhang, M. Yuan, B. Liang, Y. Li, and Y. Huangfu, "Chattering suppression fast terminal sliding mode control for aircraft EMA braking system," *IEEE Transactions on Transportation Electrification*, vol. 7, no. 3, pp. 1901–1914, 2021.

[27] B. Ding, D. Xu, B. Jiang, P. Shi, and W. Yang, "Disturbance-observer-based terminal sliding mode control for linear traction system with prescribed performance," *IEEE Transactions on Transportation Electrification*, vol. 7, no. 2, pp. 649–658, 2021.

[28] A. T. Nguyen, B. A. Basit, H. H. Choi, and J.-W. Jung, "Disturbance attenuation for surface-mounted PMSM drives using nonlinear disturbance observer-based sliding mode control," *IEEE Access*, vol. 8, pp. 86345–86356, 2020.

[29] C. Y. Lee, S. H. Hwang, E. Nam, and B. K. Min, "Identification of mass and sliding friction parameters of machine tool feed drive using recursive least squares method," *The International Journal of Advanced Manufacturing Technology*, vol. 109, no. 9–12, pp. 2831–2844, 2020.

[30] Y. Li, X. Zhang, Y. Ran, G. Zhang, and Y. Wang, "Research on meta-action decomposition and meta-action unit modeling technology for electromechanical product," *Quality and Reliability Engineering International*, vol. 36, no. 1, pp. 268–284, 2020.

[31] J. Xu, X. Li, Z. Yang, J. Su, R. Chen, and D. Shang, "Transmission friction measurement and suppression of dual-inertia system based on RBF neural network and nonlinear disturbance observer," *Measurement*, vol. 202, Article ID 111793, 2022.

[32] C. X. Wang, J. W. Tang, B. P. Jiang, and Z. T. Wu, "Sliding-mode variable structure control for complex automatic systems: a survey," *Mathematical Biosciences and Engineering*, vol. 19, no. 3, pp. 2616–2640, 2022.

[33] T. H. Nguyen, T. T. Nguyen, K. Minh Le, H. N. Tran, and J. W. Jeon, "An adaptive backstepping sliding-mode control for improving position tracking of a permanent-magnet synchronous motor with a nonlinear disturbance observer," *IEEE Access*, vol. 11, pp. 19173–19185, 2023.